

# A Novel Trenchless Detection Technology Based on Transient Electromagnetic Method for Power Poles

Lingda Xu<sup>1</sup>, Dandi Zhang<sup>2</sup>, Jun Zhou<sup>3,\*</sup>, Zhou He<sup>2</sup>, Xiao Fang<sup>2</sup> and Yonglin Zhi<sup>1</sup>

<sup>1</sup>Baisha Power Supply Bureau of Hainan Power Grid Corporation, Haikou, 570000, China

<sup>2</sup>Wuhan National High Magnetic Field Center, Huazhong University of Science and Technology, Wuhan, 430074, China

<sup>3</sup>Wuhan Second Ship Design and Research Institute, Wuhan, 430074, China

\*Corresponding Author: Jun Zhou. Email: 15827204180@163.com

**Abstract:** For the application of inspecting the construction status of distribution network poles, this paper proposed a novel detection technology for base plates, pulling plates, chucks (abbreviated as BPC) which are buried together with the power poles based on exerting external current excitation. The detection system consists of lead wires for BPC, an excitation generating circuit, a signal receiving coil, a signal conditioning circuit and an embedded processor. Compared with the traditional transient electromagnetic method, this technology is more suitable for detecting BPC which are buried shallowly, with higher sensitivity for depth changes and higher signal-to-noise ratio. Moreover, it can judge the integrity and connection condition of the BPC's metallic frameworks. The feasibility of this method is verified by simulations and experiments based on a prototype device.

**Keywords:** Formatmetal detection; nondestructive detecting; signal processing; transient electromagnetic method

## 1 Introduction

During the construction of distribution network, base plates, pulling plates, chucks (abbreviated as BPC) and stay wires are supposed to be attached to and buried with the power poles in order to keep the poles from descending and tilting. Among them, base plates, chucks and pulling plates are all concrete castings with metallic frameworks. When implementing acceptance testing, excavation will cost plenty of time and manpower. Thus, a trenchless detection method is urgently needed to judge if the BPC are set according to construction standard.

Transient electromagnetic method (TEM) is an underground metal detection method based on the principle of electromagnetic induction. It has been widely used in the fields of municipal engineering [1], tunnel prediction [2], and ore layer exploration [3-8], etc. It is a trenchless detection method with the characteristics of non-destruction and high efficiency.

The traditional TEM system normally consists of a transmitting coil and a receiving coil. When detecting, the object to be detected in deeper depth takes longer time for its returning signal to be received, thus by analyzing the receiving signals during different time period, we can get the information of the objects to be detected in different depths.

The traditional TEM has developed maturely in the application of great-depth detection. But when it comes to detecting objects in shallow ground, the returning signal (namely the secondary field signal) travels so fast that it will superpose with the signal excited by the transmitting coil (namely the primary field signal), which makes it pretty hard to recognize the secondary field signal and creates a blind zone for detection with its depth from 0 to 20 meters [9]. The buried depth of the power pole's BPC ranges from 1 to 3 meters, which lies in the blind area. Moreover, the metallic frameworks of the BPC are all small in



sizes, so the eddy-current inside are quite small too, which makes the secondary field signal even harder to be identified.

This paper proposes a novel detection method for the power pole's BPC based on exerting external excitations, which connects the excitation source with the BPC's metallic frameworks and regards them as the transmitting coils. Since this novel method deals only with the primary field signals, there is no problem of signal aliasing, and the signal strength is also greatly enhanced, making the detecting system more sensitive to the depth change of the BPC. In addition, the resistance and inductance of the BPC's metallic frameworks can be obtained by detecting the current flowing through them and the voltages on them, which can be used as a basis for evaluating the status of the BPC's frameworks.

## 2 The Power Pole System and Feasibility Analysis for the Traditional TEM

### 2.1 The Power Pole System

Fig. 1 shows the two-dimensional schematic diagram of the power pole system, which is composed of the power pole, the base plate, the chuck, the pulling plate and the stay-wire. There are various types of poles, ranging in length from 6 m to 30 m, depending on the voltage level, but all of them have spiral steel bars inside as the framework. The bottom end of the pole should be connected to the base plate in order to lower the barycenter of the whole system and to prevent the pole from descending. The chuck should be fixed on the pole with a u-shaped hoop to keep the pole from leaning to the opposite side. And the stay-wire and the pulling plate should be set on the other side to keep the pole upright. The chuck's framework is cubic, while the base plate's and the pulling plate's frameworks have only one layer. Without loss of generality, this paper will take the power pole system of 10 kV voltage class as the research object. In this situation, the length and depth of the pole are 15 m and 3 m respectively. The parameters of base plate, pulling plate and the chuck are listed in Tab. 1.

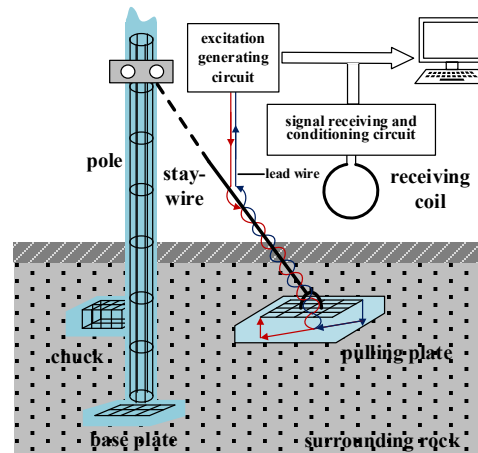


**Figure 1:** The power pole system

**Table 1:** Parameters of base plate, pulling plate and chuck

	Length (m)	Width (m)	Height (m)
Base plate	0.95	0.80	0.60
Pulling plate	0.53	0.50	0.30
Chuck	0.28	0.25	0.15

## 2.2 Feasibility Analysis for the TEM When Detecting BPC

The operating principle of TEM can be briefly described as below. Exert a fast-changing current excitation to the transmitting coil, which will induce a fast-changing magnetic field. Correspondingly, the electrical conducting objects underneath will induce eddy-currents inside them with different waveforms and amplitudes according to their depths and conductivities. The receiving coil will receive the induced voltage by the eddy-currents which we called the secondary field signal. It should be noted that the signals in the receiving coil also contains the voltage induced by the current in the transmitting coil which is called the primary field signal.

When detecting BPC with TEM, the eddy-currents induced inside the BPC's frameworks are pretty small which will result in a very small secondary field signal, due to the frameworks' hollow structure. When running a finite element method simulation in COMSOL which sets the whole system as Fig. 1 describes, the peak value of the secondary field signal induced by the base pulling plate is no more than 0.1% of the primary field signal's. And the change of the secondary field signal caused by change of pulling plate's depth is even smaller.

But considering the frameworks of BPC are all magnetic conductive, their existence will also influence the magnetic path's magnetic resistance and the mutual inductance between the transmitting coil and the receiving coil, which will eventually affect the receiving signal. Even so, the steel bars inside the pole are so much bigger than the BPC's frameworks and so much nearer to the detection system that the steel bars' influence will prevail. In conclusion, it's not appropriate for the TEM to be applied in detecting the BPC.

## 3 The Novel Detection Method Based on Exerting External Excitations

For the application in this paper, the BPC's frameworks have fixed production standards, which means there are reference values for their electrical and geometrical parameters. So when we exert a specific current excitation on one of these frameworks, the receiving signals we get are expected to be consistent with the signals got from standard BPC frameworks. If not, the tested BPC are considered failed to meet the standard and further analysis will be carried out to see the causes.

### 3.1 System Composition

As shown in Fig. 1, the system of this method is composed of excitation generating circuit, receiving coil, signal receiving and conditioning circuit, embedded processor and lead wires for the BPC. The lead wires are buried in advance during construction and used as terminals for exerting excitations. The excitation generating circuit provides excitations with specific waveforms. The receiving coil receives the electromotive force induced by the changing space magnetic field. The signal receiving and conditioning circuit is used for signal acquisition and preprocessing. The embedded processor analyzed the received signal and compare it with the theoretical signal which derives the BPC's depth and other parameters.

### 3.2 Topology of the Signal Generating Circuit

The topology of the signal generating circuit is shown in Fig. 2(a), and the BPC are equivalent to impedance models. The main circuit is composed of a battery  $U_{dc}$ , an IGBT, a BPC's framework that consists of L and  $R_1$ , a current limiting resistor  $R_2$ , and a resonance branch that contains a resistor  $R_3$  and a capacitor C. The resonance branch is added in order to gain a bigger  $di/dt$  ratio. The current limiting resistor is needed because the resistance of the framework is very small. Fig. 2(b) shows the excitation current's waveform. At time  $t_0$ , the IGBT is turned on, at time  $t_1$ , the current reaches a static value  $U_{dc}/(R_1 + R_2)$ , at time  $t_2$ , the IGBT is turned off and the current after switching off is derived as follows:

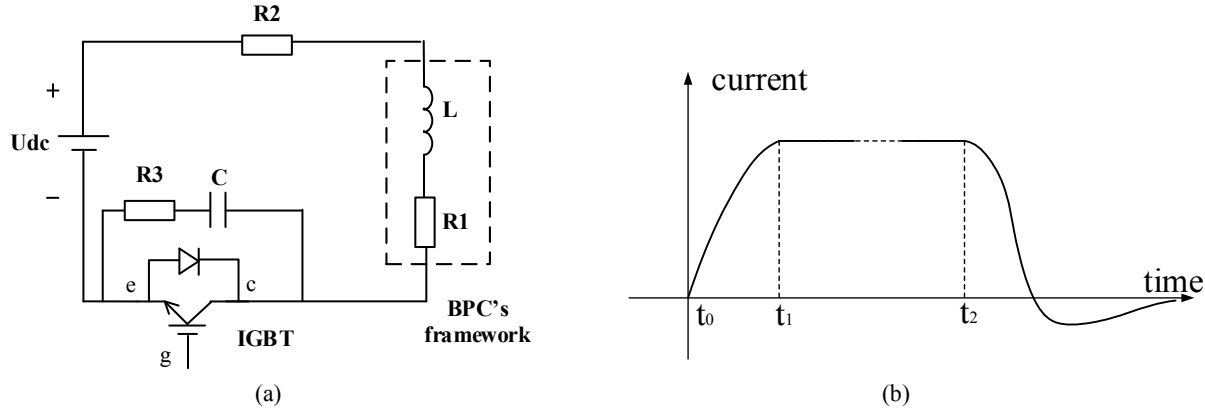


**Figure 2:** (a) signal generating circuit. (b) The excitation current's waveform

The differential equations and initial conditions:

$$\begin{cases} L \frac{di}{dt} + (R_1 + R_2 + R_3)i + u_c = U_{dc} \\ C \frac{du_c}{dt} = i, R = R_1 + R_2 + R_3 \\ u_c(0_+) = u_c(0_-) = 0 \\ i(0_+) = i(0_-) = U_{dc} / (R_1 + R_2) \end{cases} \quad (1)$$

Solve the differential equation:

$$i(t) = C\alpha e^{\alpha t} (K_1 \cos \beta t + K_2 \sin \beta t) + C e^{\alpha t} (K_2 \beta \cos \beta t - K_1 \beta \sin \beta t) \quad (2)$$

In Eq. (2),

$$\begin{aligned} K_1 = -U_{dc}, K_2 = \frac{U_{dc}}{\sqrt{4LC - R^2C^2}} \left( \frac{2L}{R_1 + R_2} - RC \right) \\ \alpha = -\frac{R}{2L}, \beta = \frac{\sqrt{4LC - R^2C^2}}{2LC} \end{aligned} \quad (3)$$

### 3.3 Operating Principle

#### 3.1.1 Depth Evaluation

The peak value of the received signal is used as the criteria for judging the BPC's depth. Since the frameworks all contain multiple rectangular meshes, the problem can be simplified, starting with studying only one excited mesh's magnetic field distribution. As shown in Fig. 3, ABCD is a rectangular mesh with current \$I\$ flowing from \$A\$ to \$C\$. \$P\$ is a point which lies on the vertical plane (namely plane PAC) of plane ABCD. The plane PAC is also the plane which the receiving coil lies on, so we only have to consider the component of the magnetic flux density at point \$P\$ which is perpendicular to plane PAC. Assuming \$AB = x\$, \$BC = y\$, \$P\$'s coordinates are \$(kx, ky)\$.

To simplify the equations below, assume that

$$\begin{aligned} PA &= \sqrt{(kx)^2 + (ky)^2 + z^2} \\ PB &= \sqrt{[(1-k)x]^2 + (ky)^2 + z^2} \\ PC &= \sqrt{[(1-k)x]^2 + [(1-k)y]^2 + z^2} \end{aligned} \quad (4)$$

The total magnetic flux density's normal component at point \$P\$ in plane PAC is

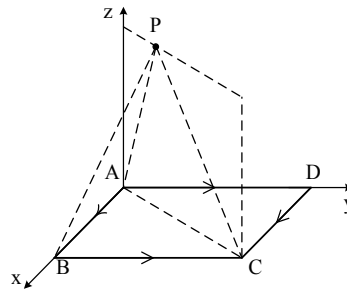


**Figure 3:** Magnetic flux density generated by one mesh

$$B_n = \frac{\mu_0 I z}{4\pi\sqrt{x^2 + y^2}} \left( \frac{kx^2}{PA \cdot [z^2 + k^2 y^2]} + \frac{ky^2}{PB \cdot [z^2 + (1-k)^2 y^2]} \right) + \frac{\mu_0 I z}{4\pi\sqrt{x^2 + y^2}} \left( \frac{(1-k)x^2}{PB \cdot [z^2 + k^2 y^2]} + \frac{(1-k)y^2}{PC \cdot [z^2 + (1-k)^2 x^2]} \right) \quad (5)$$

Consider the similarity between  $B_n$  and the magnetic flux density's normal component at point  $P$  generated by AC, which is

$$B_0 = \frac{\mu_0 I \sqrt{x^2 + y^2}}{4\pi z} \left( \frac{k}{PA} + \frac{1-k}{PC} \right) \quad (6)$$

When  $z \gg x, y$  ( $z \geq 10x, z \geq 10y$ ), a simplification can be done to  $B_n$ 's equation. In this paper, side length of the frameworks' meshes are all smaller than 15 centimeters, so the simplification is acceptable. After the simplification, the magnetic flux density's normal component at point  $P$  generated by the current in polyline ABC is

$$B_n \approx \frac{\mu_0 I}{4\pi z} \left( \frac{k \frac{x^2 + y^2}{\sqrt{x^2 + y^2}}}{PA} + \frac{(1-k) \frac{x^2 + y^2}{\sqrt{x^2 + y^2}}}{PC} \right) = \frac{\mu_0 I \sqrt{x^2 + y^2}}{4\pi z} \left( \frac{k}{PA} + \frac{1-k}{PC} \right) \quad (7)$$

Which means the magnetic flux density's normal component at point  $P$  generated by the current in polyline ABC approximately equals to which generated by the same current in line AC, so does it work with polyline ADC. So one mesh in the framework can be replaced with one diagonal line when it comes to the magnetic flux density's normal component at point  $P$  generated by it. The whole framework, taking the pulling plate's as example, can be simplified as multiple parallel lines with their currents' algebraic sum being  $I$ .

To facilitate the derivation of the relationship between signal strength and BPC's buried depth, assume the coil is in square shape, and its side length is  $l$ , the same as the length of the framework's diagonal line. The depth of the framework is  $d$ . Turns of the coil is  $N$ . The expression of the receiving coil's voltage  $U$  is as below.

$$U = \frac{N\mu_0}{4\pi} \cdot \frac{di}{dt} \left[ -2l \cdot \text{ar sinh} \left( \frac{2l}{l+2d} \right) + 2l \cdot \text{ar sinh} \left( \frac{2l}{2d-l} \right) \right] + \frac{N\mu_0}{4\pi} \cdot \frac{di}{dt} \left[ \sqrt{5l^2 + 4dl + 4d^2} - \sqrt{5l^2 - 4dl + 4d^2} - 2l \right] \quad (8)$$

The relationship between the receiving coil's voltage  $U$  and the framework's depth  $d$  is approximately exponential.

Due to multiple simplifications, such as ignoring the magnetic flux leakage and ignoring the size of the frameworks' meshes comparing to their buried depth, there may be error between the theoretical value and actual value of  $U$ , but exponential relationship between  $U$  and  $d$  is credible.

### 3.1.2 Framework's Condition Evaluation

When installing the pole system, issues like bad welding quality, metal corrosion, unreliable

connection between stay-wires and pulling plate may occur, which are potential risks for the pole system. The depth of the BPC can be judged from the  $U-d$  graph, but the issues above cannot be found if we only analyze the signal in the receiving coil. Thus the current flowing through the frameworks and the voltages on them have to be studied, from which we can derive the electrical parameters of the frameworks, namely their impedance and resistance. These can be the criteria of whether the welding quality meets the standard, whether the framework is corroded, etc.

By acquiring the static value of the voltage and current of the BPC's framework from  $t_1$  to  $t_2$ , the resistance of the framework can be calculated. And during the rising stage of the current between  $t_0$  and  $t_1$ , the inductance of the framework can be derived as below:

$$L_1 = \frac{\int_{t_0}^{t_1} u dt - R_1 \int_{t_0}^{t_1} i dt}{i(t_1) - i(t_0)} \quad (9)$$

By comparing the resistance value and inductance value with those of the standard BPC's frameworks, the condition of the tested framework can be evaluated. Moreover, the stay-wires are steel cables which are supposed to be well connected to the pulling plate, so by measuring the resistance value between the signal generating circuit's GND and the stay-wire's part on the ground, whether the stay-wire is firmly connected to the pulling plate can be judged.

## 4 Experiments

### 4.1 The Prototype Experimental Platform

To verify the feasibility of the method, a prototype experiment platform is built, which is shown in Fig. 4. A high speed 50 M AD9226 chip is selected for signal acquisition, and the architecture of the embedded processor is ARM + FPGA.

The receiving coil's diameter is 0.9 m, and its resistance  $R_3 = 5.35$  ohms, self-inductance  $L_3 = 24.468$  mH.

Taking the pulling plate's framework as the experiment object, its resistance  $R_1 = 1.608$  mohms (measured by HIOKI RM3548 RESISTANCE METER), its inductance  $L_1 = 1.0324$  uH (measured by HIOKI IM3536 LCR METER).

The current limiting resistance  $R_2 = 1$  ohms, the resonance capacitor  $C_3 = 0.22$  uF, the resonance resistor  $R_3 = 1.5$  ohms. Considering the transmission power, voltage resistance and portability, a 24 V lithium battery and a 1700 V Infineon FF300R17KE3 IGBT are selected.

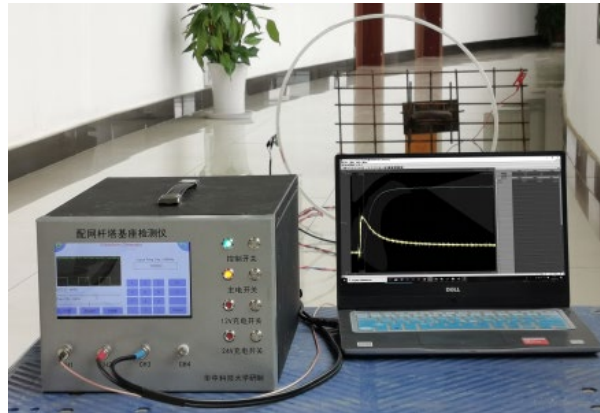


Figure 4: The prototype experiment platform

### 4.2 Verification for Depth Evaluation Function

Collecting the receiving coil's voltage data when changing the depth of the framework, the results are shown in Fig. 5. The depth ranges from 30 cm to 300 cm, which covers all of the BPC's buried depth. The relationship between the voltage's peak value  $U_r$  and the depth  $d$  is shown in Fig. 6, which is approximately

exponential and fits well with the theoretical  $Ur-d$  graph.

This means we can store the experimental data based on standard frameworks (reliably welded and not corroded) in the database, and use them as references when doing field testing to see if the tested BPC's buried depth meets the installation standard.

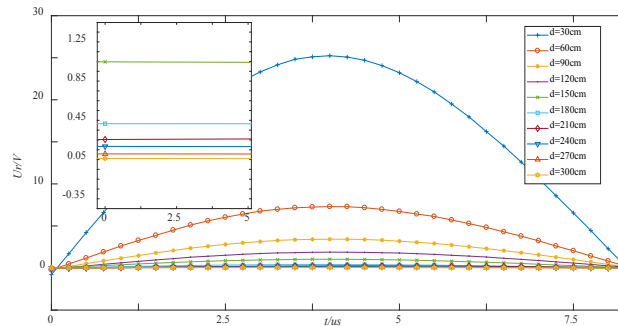


**Figure 5:** The receiving coil voltages of different framework depths

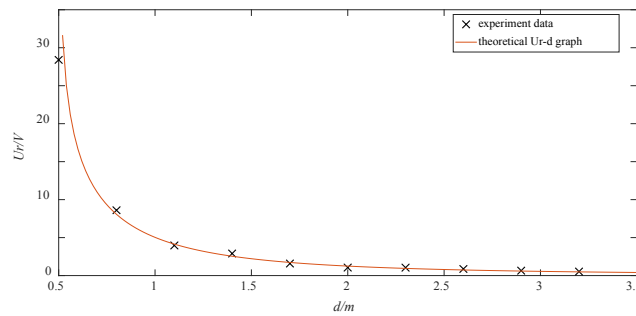


**Figure 6:** Graph of  $U$  and  $d$ 's relationship in experiments

**4.2 Verification for Structure Evaluation Function**

Fig. 7 shows the graphs of the framework's voltage and current between  $t_0$  and  $t_1$ , its resistance calculated from the experiment data is  $R_1 = 1.677$  mohms, its inductance calculated from the experiment data is  $L_1 = 0.9673$  uH, which are basically consistent with those measured by a norm-referenced instrument.

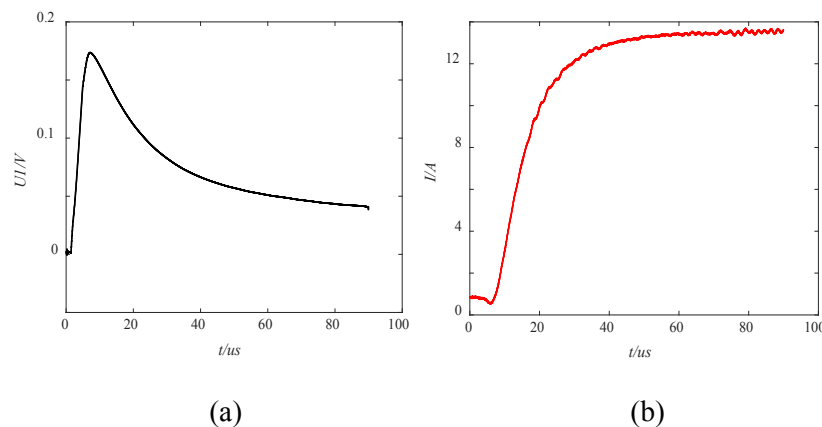


**Figure 7:** The framework's voltage and current

## 5 Conclusions

A novel method for detecting the BPC of electric poles based on exerting external excitations is proposed, which solved the signal aliasing problem of TEM when applied in BPC detecting. A prototype experimental platform is designed and build to verify the feasibility of the novel method. Experiments show that the detection scheme can detect the depth of the BPC as well as calculating their electrical parameters which can be used to evaluate the structure of them.

**Acknowledgement:** This work was supported by the National Key Research and Development Program of China under Grant 2016YFA0401702, also supported by the National Natural Science Foundation of China (51821005).

**Funding Statement:** The author(s) received no specific funding for this study.

**Conflicts of Interest:** The authors declare that they have no conflicts of interest to report regarding the present study.

## References

1. Melwaly, M., El-Qady, G., Massoud, U., El-Kenawy, A., Matsushima, J. et al. (2010). Integrated geoelectrical survey for groundwater and shallow subsurface evaluation: case study at Siliyin spring EI-Fayoum, Egypt. *International Journal of Earth Sciences*, 99(6), 1437-1436.
2. Xue, G., Yan, Y., Li, X., Di, Q. (2007). Transient electromagnetic S-inversion in tunnel prediction. *Geophysical Research Letters*, 34(18), L187403.
3. Patrick, T. S., Romain, C., Alain, R. (2015). Imaging quaternary glacial deposits and basement topography using the transient electromagnetic method for modeling aquifer environments. *Journal of Applied Geophysics*, 119, 36-50.
4. Fang, L., Gen, S. C., Wei, G. M. (2016). Transient electromagnetic detection method in water-sealed underground storage caverns. *Underground Space*, 1(1), 44-61.
5. Zhi, H. T., Yan, H. Y., Yin, G. L., Nen, S. C., Hua, J. Y. et al. (2019). Small multi-turn coils based on transient electromagnetic method for coal mine detection. *Journal of Applied Geophysics*, 169, 165-173.
6. Xue, G., Cheng, J., Zhou, N., Chen, W., Li, H. (2013). Detection and monitoring of water-filled voids using transient electromagnetic method: a case study in Shanxi, China. *Environmental Earth Sciences*, 70(5), 2263-2270.
7. Mohamed, A. K., Meju, M. A., Fontes, S. L. (2002). Deep structure of the northeastern margin of the Parnaiba Basin, Brazil, from magnetotelluric imaging. *Geophysical Prospecting*, 50(6), 589-602.
8. Mitsuhashi, Y., Uchida, T., Matsuo, K. (2006). Various-scale electromagnetic investigations of high-salinity zones in a coastal plain. *Geophysics*, 71(6), B167-B173.
9. Plotnikov, A. E. (2014). Evaluation of limitations of the transient electromagnetic method in shallow-depth studies: numerical experiment. *Russian Geology and Geophysics*, 55(7), 907-914.